Validation of Generalized State Space Averaging Method for Modeling and Simulation of Power Electronic Converters for Renewable Energy Systems

Sita R. Rimmalapudi*, Sheldon S. Williamson*, Adel Nasiri* and Ali Emadi†

Abstract – This paper presents an advanced modeling and simulation technique applied to DC/DC power electronic converters fed through renewable energy power sources. The distributed generation (DG) system at the Illinois Institute of Technology, which employs a phase-1 system consisting of a photovoltaic-based power system and a phase-2 system consisting of a fuel cell based primary power source, is studied. The modeling and simulation of the DG system is done using the generalized state space averaging (GSSA) method. Furthermore, the paper compares the results achieved upon simulation of the specific GSSA models with those of popular computer aided design software simulations performed on the same system. Finally, the GSSA and CAD software simulation results are accompanied with test results achieved via experimentation on both, the PV-based phase-1 system and the fuel cell based phase-2 power system.

Keywords: Averaging Technique, DC/DC Converters, Generalized State Space Averaging, Modeling, Renewable Energy

1. Introduction

Due to the competitive edge in power marketing and restructuring of the conventional power systems, distributed generation (DG) is becoming a much more popular practice. Following in that trend, the Illinois Institute of Technology (IIT) has set up a DG center of its own comprising of individual photovoltaic (PV) and fuel cell based power systems with batteries. It is also well known that wherever renewable energy sources such as PV and fuel cells are used for DG purposes, there exists critical power conversion circuitry in the form of DC/DC power electronic converters. The DG system at IIT uses DC/DC Boost, Buck-Boost, and Buck converters for regulating the voltage levels of the PV and fuel cell systems. Furthermore, these DC/DC converters also contribute to the maintenance of power quality in the system [1].

In DG systems, due to interconnections between different converters, a large variety of dynamic interactions are possible. If the system is defined as a large-signal model, as is required for the system level studies, linearized state space models are invalid. Time domain simulation of non-linear time-varying system modules, which includes the protection circuitry, system control dynamics, and limitations, must be used for accuracy of overall system performance simulation. Transient simulations using switching models of power electronic converters require vast computer resources and long simulation times [2].

Conventionally, averaging techniques [3]-[6] are used for the modeling of these systems. The averaged model runs much faster than the comparable switching model, and does not require excessive computer resources. However, rapid and large-signal dynamics cannot be followed by the averaging methods. Therefore, we use a generalized method in which we consider the average of the state variables as well as the harmonics. The main advantage of this large-signal approach is that there is no restriction on the size of the signal variations [7]-[9].

This paper focuses on the development of the generalized averaged models of the DC/DC converters used in conjunction with the renewable energy sources, in this case PV and fuel cells. The method adopted to achieve this is the generalized state space averaging (GSSA) method. In addition, the results of the simulations of the GSSA models, which are performed in MATLAB, are compared with computer aided design (CAD) software simulation results, which are done in the Powersim (PSIM) software. Finally, specific experimental tests were conducted on the phase-1 PV system and the phase-2 fuel cell system. The obtained output voltage waveforms are presented for the 2 systems including those for the individual DC/DC Boost, Buck-Boost, and Buck converters.

† Corresponding Author: Department of Electrical and Computer Engineering, Illinois Institute of Technology, Chicago, Illinois, USA. (emadi@iit.edu)

* Department of Electrical and Computer Engineering, Illinois Institute of Technology, Chicago, Illinois, USA.

Received 27 September, 2006 ; Accepted 25 February, 2007

2. Description of IIT's PV-Fuel Cell Hybrid DG Power System

The purpose of this project is to design and demonstrate a stand alone distributed power generation system that provides power from reliable non-polluting renewable sources to the loads. The project is conducted in two phases. Phase-1 consists of a large nickel-cadmium (Ni-Cd) battery bank that stores energy generated from a set of PV arrays. Phase-2 consists of hydrogen run fuel cell system in parallel with the Ni-Cd battery bank. Both systems are hybridized to power up a light emitting diode (LED) sign.

2.1 Phase-1 PV-Based System

Phase-1 consists of photovoltaic panels whose primary purpose is to power the load given that the sun is out. During this period, a bi-directional converter charges the batteries or supplies the grid redirecting the excess energy produced. When there is not enough power from the PV panels to run the load, battery supplies power to the load. When there is insufficient power from the PV panels and the battery bank, the grid supplies the load. A detailed schematic of the phase-1 system is depicted in Fig. 1, the various parts of which are explained below.

2.1.1 PV Array

The first set of solar panels is a 1.2kW multi-crystalline (MSX) array. Its configuration contains 20 panels in parallel tilted at a 450 angle facing south to maximize electricity output. The second set is 1kW Amorphous Millennia consisting of 33 panels in parallel tilted also at a 450 angle facing south. The maximum power output is rated at 34W per module, *Vp,max* at 60V, *Ip,max* at 4A, with an irradiance of 1000W/m2, and cell temperature of 25oC. The efficiency for the set is 10-15%.

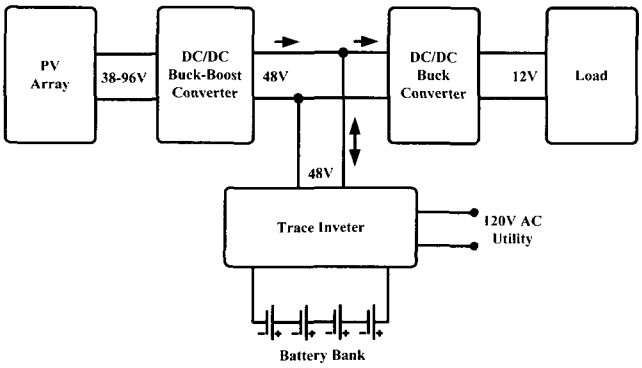

Fig 1. Schematic layout of the phase-1 of IIT's DG system.

2.1.2 Charge Controller

Each set of solar panels is connected separately to charge controllers, which are essentially DC/DC Buck-Boost converters. The "Trace Engineering C-40" charge controllers generate 40A of current from the PV array and maintain a voltage of 48V DC to charge the battery bank. The maximum current rating of the charge controller is 63A. The charge controller optimizes the performance of the battery bank by regulating the output current from the solar panels and the input current to the battery bank.

2.1.3 Load

The load profile is composed of an LED display electrical sign. The peak power requirement of the sign is rated at 450W, when all bulbs are lit. On an average, however, the output is considerably less depending on the message displayed on the sign.

2.1.4 Battery Bank

There are 38 Nickel-Cadmium batteries that are specifically designed for the photovoltaic systems. These 38 cells are connected in series to provide an output battery voltage of 48V. The cell capacity is measured by the amount of electrical energy stored. The product of current discharged from the cell and the time for which the current is sustained before the fall of voltage results in the total capacity of the cell. The capacity of used batteries is rated at 300A-h. The total available energy from the battery bank is estimated at 13.68kWh.

2.2 Phase-2 Fuel Cell Based System

In Phase 2, a 300W proton exchange membrane (PEM) fuel cell is used to power the load via series connected DC/DC Boost converter and DC/DC Buck converter. Varying voltage characteristic of the fuel cell necessitates a Boost converter that supplies constant 48V output. A detailed schematic of phase-2 is depicted in Fig. 2, the various parts of which are explained below.

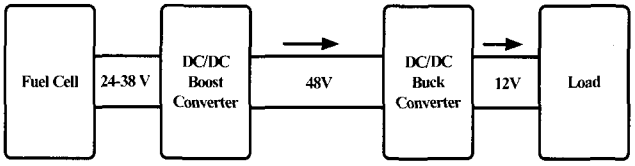

Fig. 2. Schematic layout of the phase-2 of IIT's DG system.

2.2.1 Proton Exchange Membrane (PEM) Fuel Cell

This is a 300W air breathing PEM fuel cell from "H Power Corp." Major specifications are shown in Table 1 below.

2.2.2 DC/DC Input Boost Converter

This converter gives a constant output voltage irrespective of the input voltage from the fuel cell. Fuel cell voltage typically varies between 24 to 38V depending upon the output current. This is because of the polarization effect of the cell stack [1].

Table 1. PEM fuel cell specifications.

Manufacturer	H Power
Type	PEM
Membrane	Polymer electrolyte
Reactants	Hydrogen and air
Open Circuit Voltage	36V
Operating Voltage	27.5V at 11 Amp
Operating Current	11A Nominal, 14A max.
Rated Power Output at 11A	302.5W
Peak Power	375W at 14A

3. Generalized State Space Averaging (GSSA) Method

Generalized state space averaging method is based on the fact that the waveform $x(t)$ can be approximated with arbitrary precision in the $(t\text{-}T, t)$ range by a Fourier series expansion [7]-[9]. This is given by:

$$x(t) = \sum_{k=-n}^{n} < x >_k (t) e^{jk\omega t} \tag{1}$$

where

$$\omega = \frac{2\pi}{T}$$

$$< x >_k (t) = \frac{1}{T} \int_{t-T}^{t} x(\tau) e^{-jk\omega\tau} d\tau \tag{2}$$

In the equation (1), the value of n depends on the required degree of accuracy; if n approaches infinity, the approximation error approaches zero. If we only consider the term $K=0$, we have the same state space averaging method [3]-[6]. If a state variable does not have an oscillating form and is almost constant, we only use the term $K=0$. In addition, if a state variable only has an oscillating form similar to a sine wave, we use the terms $K=-1,1$. This method is named first harmonic approximation. Furthermore, if a state variable has a DC coordinate, also has an oscillating form, we use the terms $K=-1,0,1$. However, more terms we consider more accuracy we have.

Selection of T for modeling of each converter is very important, which should be considered carefully. For instance, it is the switching period in DC/DC converters and the main wave period of the output voltage in DC/AC inverters. Here, $< x >_k (t)$ is complex Fourier coefficient. These Fourier coefficients are functions of time since the interval under consideration slides as a function of time. The analysis computes the time-evolution of these Fourier coefficients as the window of length T slides over the actual waveform. Our approach is to determine an appropriate state space model in which the coefficients (2) are the state variables.

4. GSSA Applied to DG-Based Power Electronic System

In this section, a modular approach for the modeling of power electronic converters using generalized state space averaging method is discussed. The converters and subsystems of the system are modularised and subsequently interconnected to form the complete system [9]. Modularising the system into converters and subsystems has several advantages: (1) converters and subsystems models can be used in different systems; (2) it reduces the complexity of modeling large systems by modeling a less complex subsystem; and (3) the proposed models can be verified with manageable test conditions.

4.1 DC/DC Converters in DG systems

We suppose that the converters that are to be discussed in subsequent sections, i.e., Buck, Boost, or Buck-Boost converters, are operating in continuous conduction mode (CCM) with switching period T and duty cycle d. To apply the generalized state space averaging method, commutation function $u(t)$ is defined as

$$u(t) = \begin{cases} 1, 0 < t < dT \\ 0, dT < t < T \end{cases} \tag{3}$$

This commutation function depends on the circuit switching control, which determines when the circuit topology changes according to time.

4.1.1 Buck Converter

Fig. 3 shows a DC/DC PWM Buck converter. Input side of the converter is connected to either fuel cell system or PV system. Output is connected to the load. The unified set of circuit state variable equations, in continuous conduction mode of operation, is obtained by applying (3) to the two sets of topological circuit state space equations.

Nevertheless, in the set of equations of the generalized state space averaged model, the actual state space variables are the Fourier coefficients of the circuit state variables which are, in this case, i_L and v_o.

$$\begin{cases} \dfrac{di_L}{dt} = \dfrac{1}{L}\left[v_{in}u(t) - v_o\right] \\ \dfrac{dv_o}{dt} = \dfrac{1}{C}\left[i_L - i_{out}\right] \\ i_{in} = i_L u(t) \end{cases} \tag{4}$$

Using the first-order approximation to obtain i_L and v_o, we have six real state variables as follows.

$$\begin{aligned} &< i_L >_0 = x_1, < v_o >_0 = x_2 \\ &< i_L >_1 = x_3 + jx_4, < v_o >_1 = x_5 + jx_6 \end{aligned} \tag{5}$$

Since i_L and v_O are real,

$$< i_L >_{-1} = < i_L >_1^*, < v_o >_{-1} = < v_o >_1^* \tag{6}$$

where the operator * means the conjugate of a complex number. The circuit state variables are calculated and given by

$$\begin{aligned} i_L(t) &= x_1 + 2x_3 Cos\omega t - 2x_4 Sin\omega t \\ v_o(t) &= x_2 + 2x_5 Cos\omega t - 2x_6 Sin\omega t \end{aligned} \tag{7}$$

By applying the time derivative property of the Fourier coefficients in (4), and further substituting the Fourier coefficients of the communication function $u(t)$

$$< u(t) >_0 = d, < u(t) >_1 = \frac{j}{2\pi}(e^{-j2\pi d} - 1) \tag{8}$$

One comes to

$$\begin{bmatrix} \dot{x}_1 \\ \dot{x}_2 \\ \dot{x}_3 \\ \dot{x}_4 \\ \dot{x}_5 \\ \dot{x}_6 \end{bmatrix} = \begin{bmatrix} 0 & \frac{1}{L} & 0 & 0 & 0 & 0 \\ \frac{1}{C} & \frac{1}{RC} & 0 & 0 & 0 & 0 \\ 0 & 0 & 0 & \omega & \frac{1}{L} & 0 \\ 0 & 0 & -\omega & 0 & 0 & \frac{1}{L} \\ 0 & 0 & \frac{1}{C} & 0 & \frac{1}{RC} & \omega \\ 0 & 0 & 0 & \frac{1}{C} & -\omega & \frac{1}{RC} \end{bmatrix} * \begin{bmatrix} x_1 \\ x_2 \\ x_3 \\ x_4 \\ x_5 \\ x_6 \end{bmatrix} + \begin{bmatrix} \frac{dV_{in}}{L} \\ 0 \\ \frac{V_{in}\sin 2\pi d}{2\pi L} \\ \frac{-V_{in}(1-\cos 2\pi d)}{2\pi L} \\ 0 \\ 0 \end{bmatrix} \tag{9}$$

Equation (9) is the generalized state space averaged model of the Buck converter.

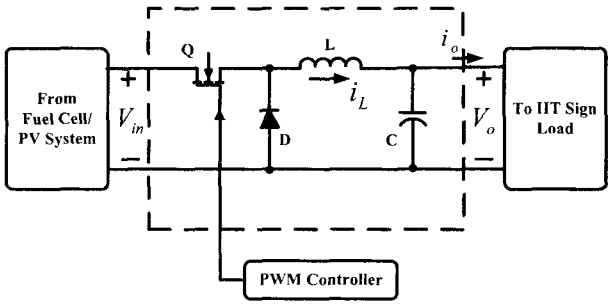

Fig. 3. DC/DC PWM buck converter.

4.1.2 Boost Converter

Fig. 4 shows a DC/DC PWM Boost converter. Input side of the converter is connected to the PEM fuel cell. Output is connected to a 48V bus and to a Buck converter. The unified set of circuit state variable equations, in continuous conduction mode of operation, is obtained by applying (3) to the two sets of topological circuit state space equations [9].

$$\begin{cases} \dfrac{di_L}{dt} = \dfrac{1}{L}\left[v_{in} - (1-u(t))v_o\right] \\ \dfrac{dv_o}{dt} = \dfrac{1}{C}\left[(1-u(t))i_L - i_{out}\right] \\ i_{in} = i_L \end{cases} \tag{10}$$

By applying the generalized state space averaging method, as was presented for the Buck converter, state space equations of the converter can be written as

$$\begin{bmatrix} \dot{x}_1 \\ \dot{x}_2 \\ \dot{x}_3 \\ \dot{x}_4 \\ \dot{x}_5 \\ \dot{x}_6 \end{bmatrix} = \begin{bmatrix} 0 & \frac{d-1}{L} & 0 & 0 & \frac{\sin 2\pi d}{\pi L} & \frac{-(1-\cos 2\pi d)}{\pi L} \\ \frac{1-d}{C} & \frac{1}{RC} & \frac{-\sin 2\pi d}{\pi C} & \frac{1-\cos 2\pi d}{\pi C} & 0 & 0 \\ 0 & \frac{\sin 2\pi d}{2\pi L} & 0 & \omega & \frac{d-1}{L} & 0 \\ 0 & \frac{-(1-\cos 2\pi d)}{2\pi L} & -\omega & 0 & 0 & \frac{d-1}{L} \\ \frac{-\sin 2\pi d}{2\pi C} & 0 & \frac{1-d}{C} & 0 & \frac{1}{RC} & \omega \\ \frac{1-\cos 2\pi d}{2\pi C} & 0 & 0 & \frac{1-d}{C} & -\omega & \frac{1}{RC} \end{bmatrix} * \begin{bmatrix} x_1 \\ x_2 \\ x_3 \\ x_4 \\ x_5 \\ x_6 \end{bmatrix} + \begin{bmatrix} \frac{V_{in}}{L} \\ 0 \\ 0 \\ 0 \\ 0 \\ 0 \end{bmatrix} \tag{11}$$

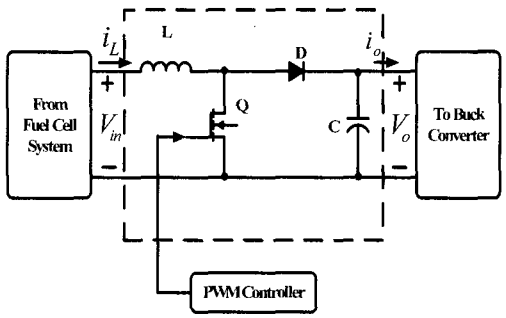

Fig. 4. DC/DC PWM Boost converter.

4.1.3 Buck-Boost Converter

Fig. 5 shows a DC/DC PWM Buck-Boost converter. Input side of the converter is connected to the PV system. Output is connected to a 48V bus and a Buck converter. The unified set of circuit state variable equations, in continuous conduction mode of operation, is obtained by applying (3) to the two sets of topological circuit state space equations [9].

$$\begin{cases} \dfrac{di_L}{dt} = \dfrac{1}{L}\left[v_{in}u(t) - (1-u(t))v_o\right] \\ \dfrac{dv_o}{dt} = \dfrac{1}{C}\left[(1-u(t))i_L - i_{out}\right] \\ i_{in} = i_L u(t) \end{cases} \tag{12}$$

By applying the generalized state space averaging method, as was presented for the DC/DC Buck converter, state space equations of the converter can be written as:

$$\begin{bmatrix} \dot{x}_1 \\ \dot{x}_2 \\ \dot{x}_3 \\ \dot{x}_4 \\ \dot{x}_5 \\ \dot{x}_6 \end{bmatrix} = \begin{bmatrix} 0 & \frac{d-1}{L} & 0 & 0 & \frac{\sin 2\pi d}{\pi L} & \frac{-(1-\cos 2\pi d)}{\pi L} \\ \frac{1-d}{C} & \frac{1}{RC} & \frac{-\sin 2\pi d}{\pi C} & \frac{1-\cos 2\pi d}{\pi C} & 0 & 0 \\ 0 & \frac{\sin 2\pi d}{2\pi L} & 0 & \omega & \frac{d-1}{L} & 0 \\ 0 & \frac{-(1-\cos 2\pi d)}{2\pi L} & -\omega & 0 & 0 & \frac{d-1}{L} \\ \frac{-\sin 2\pi d}{2\pi C} & 0 & \frac{1-d}{C} & 0 & \frac{1}{RC} & \omega \\ \frac{1-\cos 2\pi d}{2\pi C} & 0 & 0 & \frac{1-d}{C} & -\omega & \frac{1}{RC} \end{bmatrix} * \begin{bmatrix} x_1 \\ x_2 \\ x_3 \\ x_4 \\ x_5 \\ x_6 \end{bmatrix} + \begin{bmatrix} \frac{dV_{in}}{L} \\ 0 \\ \frac{V_{in}\sin 2\pi d}{2\pi L} \\ \frac{-V_{in}(1-\cos 2\pi d)}{2\pi L} \\ 0 \\ 0 \end{bmatrix} \tag{13}$$

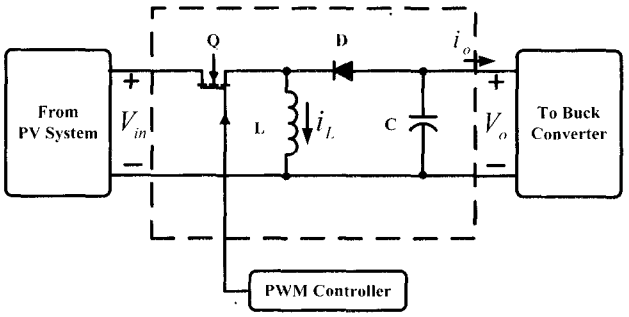

Fig. 5. DC/DC PWM Buck-Boost converter.

5. Summary of GSSA and CAD Simulation (PSIM) Simulation Results

In order to support the simulation results of the GSSA models for the PV and fuel cell based buck, boost, and buck-boost converters, CAD simulations were performed in the PSIM software. It is worthwhile mentioning here that the obtained results were identical to those of the modeled converters.

In this section, the comparative results of each simulation performed on the specific DC/DC converters are presented. Firstly, the PV-based DC/DC Buck-Boost converter is simulated in PSIM and the corresponding output voltage and inductor currents are obtained under steady-state operating conditions. Thereafter, the fuel cell based DC/DC Boost converter is simulated and the resulting voltage and current waveforms are presented. Lastly, the PV-based DC/DC Buck converter is simulated, using a DC voltage of 48V as its input, and the associated steady-state voltage and current waveforms are recorded. In addition, the simulation results of the entire fuel cell system comprising of the DC/DC input Boost converter and the DC/DC output Buck converter are also presented. As mentioned before, the simulation results possess very similar characteristics and are as shown in Figs. 6-9.

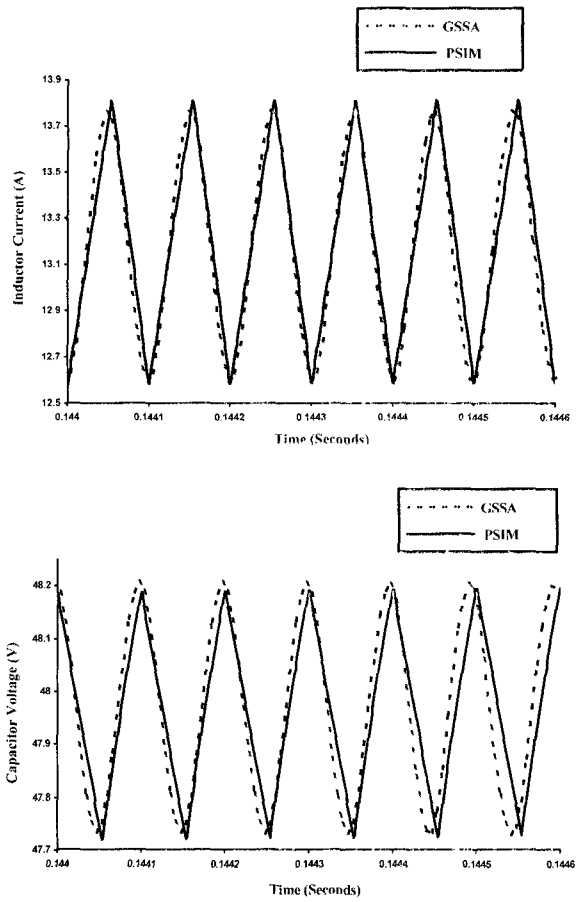

Fig. 6. Comparative simulation results of PV-based DC/DC Buck-Boost converter.

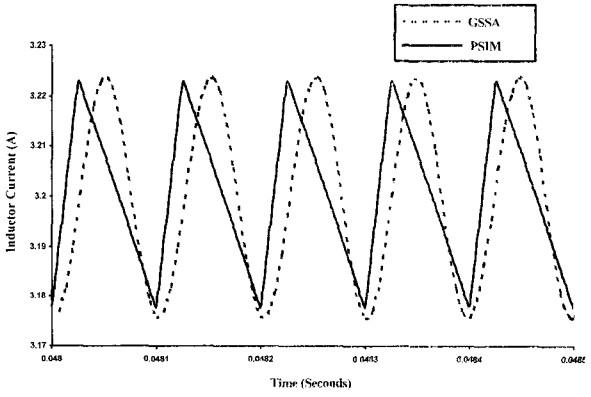

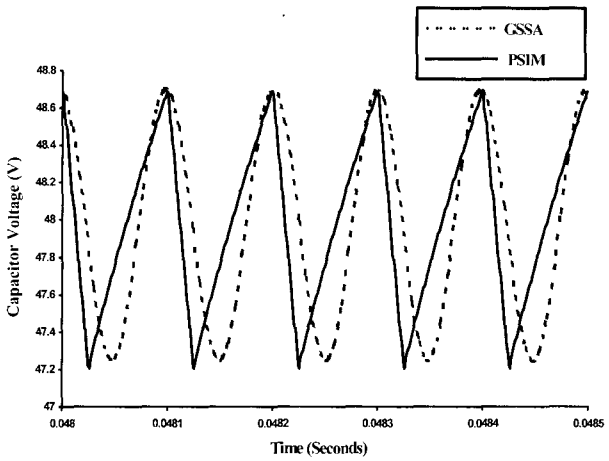

Fig. 7. Comparative simulation results of fuel cell based DC/DC Boost converter.

It is worthwhile mentioning here that the PV-based system simulation generated similar results to those of the DC/DC Buck converter. This is because of the hybridized 48V battery storage system that is connected in parallel with the PV system. Thus, the simulation results of the entire PV system are primarily the same as those of the DC/DC Buck converter with a constant input voltage of 48V DC. Thus, no extra simulation work was involved.

As can be clearly observed from Figs. 6-9, the simulation results for the steady state output voltage and inductor current waveforms, for the various DC/DC converters, employed in accordance with the PV and fuel cell based power systems, show distinct similarities for both the GSSA models as well as the PSIM schematics.

The original voltage values aimed were 48V for the DC/DC PV-based Buck-Boost and fuel cell based Boost converters and 12V for the respective output DC/DC Buck converters. These values are precisely achieved, via the simulation of the GSSA models (in MATLAB) and the CAD software schematic systems (in PSIM). Furthermore, as is clear from Figs. 6-9, there exists not much variation from the averaged value of voltage or current, achieved via the simulations, thus suggesting that the GSSA technique is indeed a powerful tool for simulating power electronic converters for DG applications, such as the one considered in this case. To present a brief idea of the accuracy of results, obtained via GSSA modeling and PSIM simulations, there exists a minor variation of 0.6-0.8% between the values of specific DC/DC converter voltages and currents upon comparison of the actual data obtained from the two simulation procedures.

In addition, it is worthwhile to point out that the GSSA modeling results obtained here is via the first order approximation. If higher order approximations are used, the corresponding model matrices have greater number of state variables, for the specific DC/DC converter. However, obviously at the same time, the model accuracy improves appropriately. Thus, the entire modeling process involves a distinct trade-off between complexity of calculations and higher model accuracy.

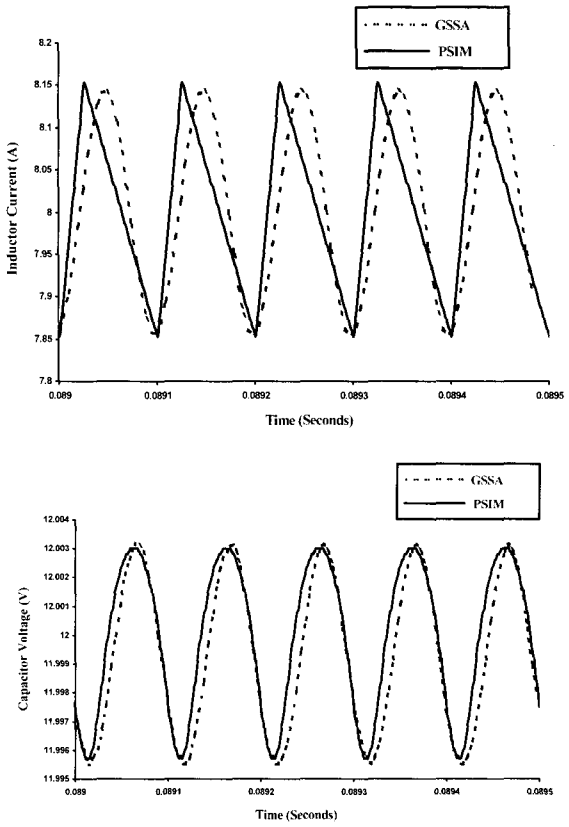

Fig. 8. Comparative simulation results of PV system output DC/DC Buck converter.

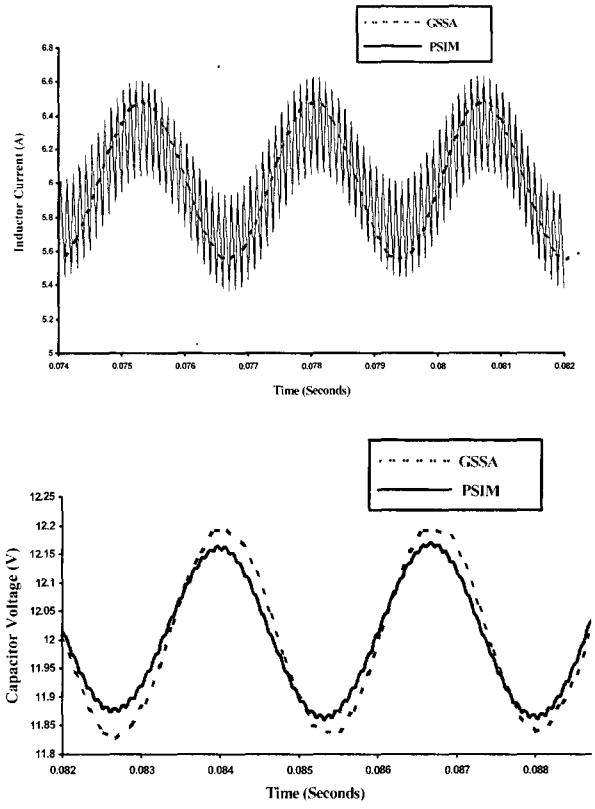

Fig. 9. Comparative simulation results of fuel cell system output DC/DC Buck converter

6. Experimental Setup and Test Results

Control room setup of PV-based DG system is shown in Fig. 10. PV arrays (not shown in the picture) are installed on the roof. The PV panels are connected to the DC/DC Buck-Boost converter through a disconnect switch.

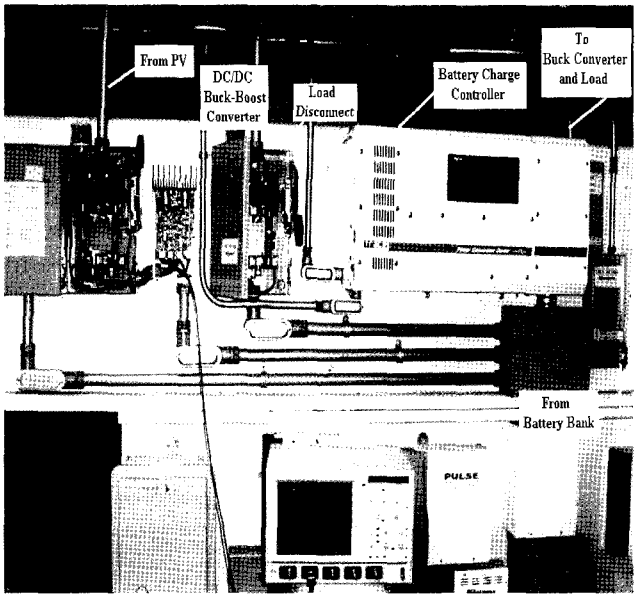

Fig 10. Pictorial representation of the PV-based power system.

As is visible in the pictorial view of the PV system shown in Fig. 10, the PV system is connected in parallel with the secondary battery energy storage system. In fact, the battery storage system is not visible in this picture since it is placed external to the PV system control room. Voltage waveform at the output terminal of the Buck-Boost converter is observed and is shown in Fig. 11. It is worthwhile mentioning here that the peak-to-peak variation in output voltage is approximately 0.48V.

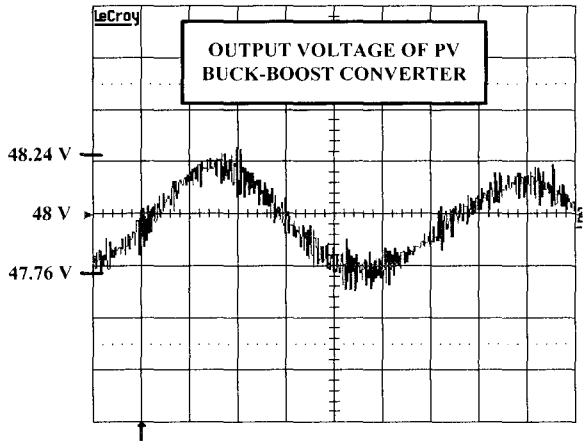

Fig. 11. Steady state voltage waveform of the PV Buck-Boost converter.

Experimental set-up of the fuel cell system is shown in Fig. 12. Industrial grade hydrogen is used to fuel the PEM fuel cell. Secondary reactant, oxygen, is absorbed from the atmosphere. Output voltage of the PEM fuel cell is stabilized to 48V by the DC/DC Boost converter. Steady state output voltage waveform ripple is shown in Fig. 13. Thereafter, the role of the DC/DC Buck converter is to step down the voltage to 12V from 48V. The steady state output voltage waveform is shown in Fig. 14.

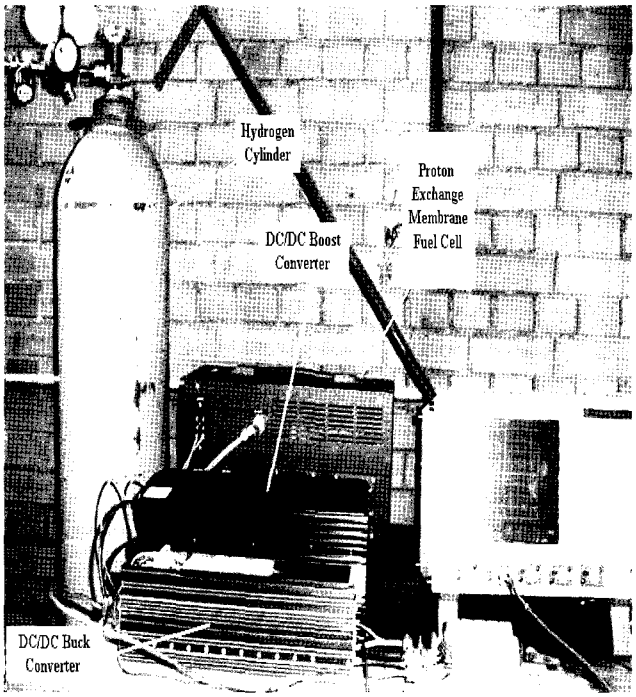

Fig. 12. Pictorial representation of PEM fuel cell system.

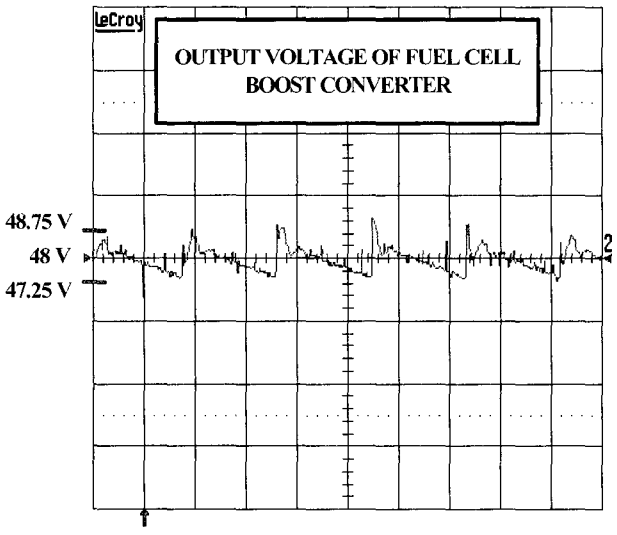

Fig. 13. Steady state output voltage waveform of the fuel cell boost converter.

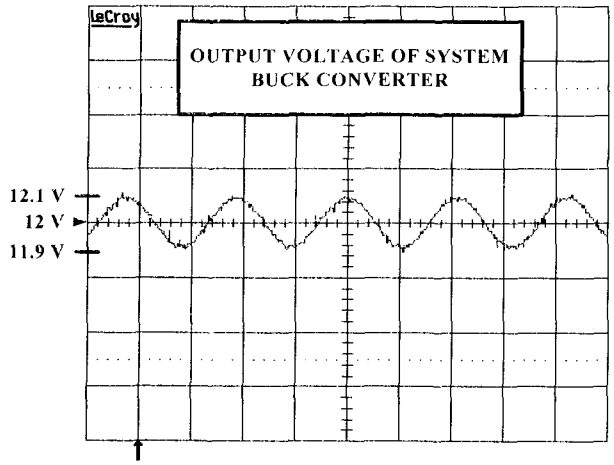

Fig. 14. Steady state output voltage waveform of the system Buck converter.

It is interesting to note that the variations in steady state output voltage for the fuel cell based DC/DC Boost converter, as shown in Fig. 13, appears to be much more than the other two converter topologies. But in reality, the total value of variation is not much different from those of the other cases. Furthermore, the overall system output voltage waveform, as shown in Fig. 14, shows much smoother characteristics although its peak-to-peak variations were obviously recorded to be slightly higher. This is due to the fact that the entire system dynamics are considered in this case, which in turn, affects the variations in steady state voltage waveform.

For the next phase of IIT's DG system, as is shown in Fig. 15, the two existing PV and fuel cell systems will be connected together. An important issue to be taken care of while performing the simulations and experimental studies on this system would be the system dynamics due to the hybridization of the fuel cell system along with the PV and battery storage systems. In addition, this topology distinctly reduces the number of DC/DC power electronic converters involved and, hence, facilitates much more cost reduction and system complexities.

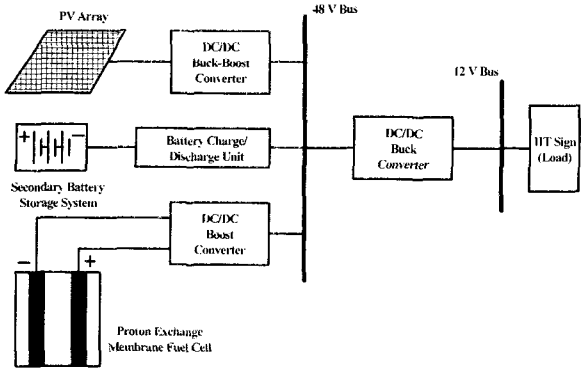

Fig. 15. Proposed DG system topology for future development work.

7. Conclusion

This paper has primarily presented the modeling and simulation of DC/DC converters working in conjunction with PV and fuel cell based distributed generation (DG) systems. The method adopted to achieve this was the generalized state space averaging (GSSA) technique. In addition, the results of the simulation of these GSSA DC/DC converter models, which were performed in MATLAB, were compared with computer aided design (CAD) software simulation results, which were executed in the Powersim (PSIM) software. The results of the GSSA modeling and the PSIM simulations had fairly similar characteristics. Finally, specific experimental tests were conducted on the phase-1 PV system and the phase-2 fuel cell system. The obtained output voltage waveforms were presented for the two systems including those for the individual DC/DC Boost, Buck, and Buck-Boost converters. The experimental results also showed similar values to those of the modeled systems under steady state operating conditions thus proving the viability of the GSSA modeling technique for renewable energy systems.

Acknowledgement

Support of Dr. Said-Al-Hallaj of the Center for Electrochemical Science and Engineering at Illinois Institute of Technology is gratefully acknowledged.

References

[1] S. Chowdary, B. Wilson, S. Al-Hallaj, and D. Chmielewski, "Active control of a hybrid fuel cell – battery system", in *Proc. 203rd Electrochemical Society Meeting*, Paris, France, April 2003.

[2] A. Emadi, "Modeling, analysis, and stability assessment of multi-converter power electronic systems", *Ph.D. Dissertation,* Texas A&M University, College Station, TX, Aug. 2000.

[3] R. D. Middlebrook and S. Cuk, "A general unified approach to modeling switching converter power stages", in *Proc. IEEE Power Electronics Specialist Conf.*, June 1976, pp. 18-34.

[4] P. T. Krein, J. Bentsman, R. M. Bass, and B. Lesieutre, "On the use of averaging for the analysis of power electronic systems", *IEEE Trans. on Power Electronics*, vol. 5, no. 2, pp. 182-190, 1990.

[5] J. Sun and H. Grotstollen, "Averaged modeling of switching power converters: reformulation and theoretical basis", in *Proc. IEEE Power Electronics Specialist Conf.*, June 1981, pp. 1165-1172.

[6] G. Verghese and U. Mukherdji, "Extended averaging

and control procedure", in *Proc. IEEE Power Electronics Specialist Conf.*, June 1981, pp. 329-336.

[7] S. R. Sanders, J. M. Noworoski, X. Z. Liu, and G. C. Verghese, "Generalized averaging method for power conversion circuits", *IEEE Trans. on Power Electronics*, vol. 6, no. 2, April 1991.

[8] J. Mahdavi, A. Emadi, M. D. Bellar, and M. Ehsani, "Analysis of power electronic converters using the generalized state space averaging approach", *IEEE Trans. on Circuits and Systems I: Fundamental Theory and Applications*, vol. 44, no. 8, Aug. 1997.

[9] A. Emadi, "Modeling and analysis of multiconverter DC power electronic systems using the generalized state space averaging method", *IEEE Transactions on Industrial Electronics,* vol. 51, no. 3, pp. 661-668, June 2004.

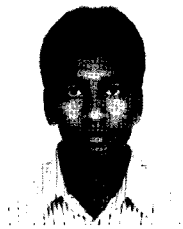

Sita R. Rimmalapudi

He received his M.S. degree in electrical engineering from Illinois Institute of Technology (IIT), Chicago, USA, in December 2003. He was a graduate research assistant in Grainger Power Electronics and Motor Drives Laboratory at IIT. He is currently with Aviation Instrument Tech Inc. in Zephyrhills, Florida, USA.

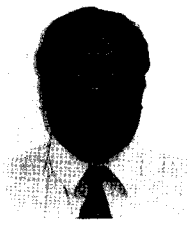

Sheldon S. Williamson

He received his Bachelor of Engineering (B.E.) degree in Electrical Engineering with high distinction from Bombay University, India, in 1999. He received the Master of Science (M.S.) degree in 2002, and the Doctor of Philosophy (Ph.D.) degree in 2006, both in Electrical Engineering, from the Illinois Institute of Technology, Chicago, IL, majoring in power electronics and motor drives at the Grainger Power Electronics and Motor Drives Laboratory. During 2001-2006, he was with the Electric Power and Power Electronics Center, at the Illinois Institute of Technology. He is currently an assistant professor at Concordia University in Canada. He has authored/co-authored over 20 journal and conference papers. In addition, he has offered numerous conference tutorials, lectures, and short courses in the areas of Automotive Electronics and Vehicular Power Systems. His current research interests involve the study and analysis of hybrid electric and fuel cell vehicular power systems.

Dr. Williamson is the recipient of the Paper of the Year Award in 2006 in the field of Automotive Electronics from the IEEE Vehicular Technology Society (IEEE VTS). He also received the prestigious Sigma Xi/IIT Award for Excellence in University Research for the academic year 2005-2006. He is also the recipient of the 2006 Best Research Student Award, Ph.D. category, in the ECE Department, at the Illinois Institute of Technology. He is a Member of the IEEE and SAE.

Adel Nasiri

He was born in Sari, Iran, in 1974. He received the B.S. and M.S. degrees from Sharif University of Technology, Tehran, Iran, in 1996 and 1998, respectively, and the Ph.D. degree from Illinois Institute of Technology, Chicago, Illinois, in 2004, all in electrical engineering.

He worked for Moshanir Power Engineering Company, Tehran, Iran, from 1998 to 2001. He also worked for ForHealth Technologies, Inc., Daytona Beach, Florida, from 2004 to 2005 on an automated syringe filling device. Dr. Nasiri is presently an Assistant Professor in the Department of Electrical Engineering and Computer Science at the University of Wisconsin–Milwaukee, where he is the director of power electronics and motor drives laboratory. His research interests are power electronics converters, uninterruptible power supplies, renewable energy systems, and electric motor controls.

Ali Emadi

He is a professor of electrical engineering and the director of the Electric Power and Power Electronics Center at Illinois Institute of Technology (IIT), where he has established research and teaching facilities as well as courses in power electronics, motor drives, and vehicular power systems. Dr. Emadi is the founder, director, and chairman of the board of the Industry/Multi-university Consortium on Advanced Automotive Systems (IMCAAS). He is also the founder and Chief Technology Officer (CTO) of Hybrid Electric Vehicle Technologies, Inc.

Dr. Emadi is the recipient of numerous awards and recognitions. He has been named the Eta Kappa Nu Outstanding Young Electrical Engineer of the Year 2003 by virtue of his outstanding contributions to hybrid electric vehicle conversion. He also received the 2005 Richard M. Bass Outstanding Young Power Electronics Engineer Award from the IEEE Power Electronics Society. Dr. Emadi is the recipient of the 2002 University Excellence in Teaching Award from IIT as well as the 2004 Sigma Xi/IIT Award for Excellence in University Research. He directed a team of students to design and build a novel motor drive, which won the First Place Overall Award of the 2003 IEEE/DOE/DOD International Future Energy Challenge for Motor Competition.

Dr. Emadi was the General Chair of the 2005 IEEE Vehicle Power and Propulsion and SAE Future Transportation Technology Joint Conference. Dr. Emadi is the author/co-author of over 200 journal and conference papers as well as several books including *Vehicular Electric Power Systems* (Marcel Dekker, 2003), *Energy Efficient Electric Motors* (Marcel Dekker, 2004), *Uninterruptible Power Supplies and Active Filters* (CRC Press, 2004), and *Modern Electric, Hybrid Electric, and Fuel Cell Vehicles* (CRC Press, 2004). He is also the editor of the *Handbook of Automotive Power Electronics and Motor Drives* (Marcel Dekker, 2005).